Patient-Derived Organotypic Tumor Spheroids Facilitate Precision Medicine Advances in Therapeutic Screening for Malignant Pleural Mesothelioma

Table of Contents

Glossary

AOPI Solution	Acridine orange, propidium iodide
BAP1	BRCA1-associated protein 1 gene
CT	Computed tomography
CTC	Circulating tumor cells
CTLA-4	Cytotoxic T-Lymphocyte Associated Protein 4
DMEM	Dulbecco's Modified Eagle Medium
EMT	Epithelial-mesenchymal transition
EPP	Extrapleural pneumonectomy
FBS	Fetal bovine serum
FcR	Fc receptor
HEPES	4-(2-hydroxyethyl)-1-piperazineethanesulfonic acid
ICB	Immune checkpoint blockade
ICI	Immune checkpoint inhibitor
IMRT	Intensity-modulated radiation therapy
MM	Malignant mesothelioma
MCR	Macroscopic complete resection
MPM	Malignant pleural mesothelioma
NaOH	Sodium hydroxide
PBS	Phosphate-buffered saline
PBST	Phosphate-buffered saline with Tween 20
PD	Progressive disease
P/D	Pleurectomy and decortication
PD-1	Programmed cell death protein 1
PD-L1	Programmed death-ligand 1
PDMS	Polydimethylsiloxane
PDOTS	Patient-derived organotypic tumor spheroids
PDX	Patient-derived xenograft
PET	Positron emission tomography
PR	Partial response
RPMI	Roswell Park Memorial Institute medium
RT	Radiotherapy or radiation therapy
SD	Stable disease
SMRP	Soluble mesothelin-related peptide
STAT3	Signal transducer and activator of transcription 3
SV40	Simian virus 40
TME	Tumor microenvironment
TMT	Trimodality therapy
VEGF	Vascular endothelial growth factor

Acknowledgements

I would like to express my sincere gratitude to all individuals who made this research possible. First, I would like to thank my advisor, Dr. Raphael Bueno, who welcomed me into his lab with open arms and enthusiastically provided me with the opportunity to learn more about thoracic diseases. In addition, I would like to express my deepest appreciation to Dr. Cloud Paweletz, who guided me through this work and taught me not only about scientific inquiry but also about the importance of acting on our ideas, even when they may be imperfect. Lastly, this work would not have come to fruition without the mentorship of Dr. David Barbie who extended his support and provided invaluable advice throughout this project.

Within the Belfer Center for Applied Cancer Science, I extend a very special thank you to Dr. Elena Ivanova who always offered me her guidance and friendship without reservation. It was also a privilege to learn from and be mentored by Dr. Amir Aref who was an outstanding teacher from day one. Separately, within the Thoracic Surgery Oncology Laboratory, I am very thankful for the guidance of Dr. Assunta De Rienzo who took me under her wing on many occasions and taught me so much about mesothelioma. Similarly, I thank Dr. William "Bill" Richards who patiently helped me think through challenging aspects of this work and always provided helpful discussions. Finally, I am very appreciative for the encouragement and support of the following lab members and research assistants: Andrew Portell, Brandon Piel, and Claire Meyerovitz.

Ultimately, this work would not be possible without the help of the Division of Thoracic Surgery, the Thoracic Surgery Oncology Laboratory, and the International Mesothelioma Program at Brigham and Women's Hospital. A sincere thank you to everyone.

Abstract

Malignant pleural mesothelioma (MPM) is an aggressive cancer with limited curative treatment, common tumor recurrence, and poor prognosis. Given the fatal nature of this disease and limited effectiveness of conventional therapies, novel approaches to treatment are essential. To this end, in prior research we demonstrated that utilization of 3D microfluidic cell culture in combination with patient-derived organotypic tumor spheroids (PDOTS) can serve as a model to study the tumor microenvironment and cellular responses to treatment in cancer. Through this study, we pursued three aims: (1) evaluate pre-analytical variables from the operating room to the lab bench predicted to have an effect on generation of PDOTS; (2) perform short term comparative analysis of tumor responses to standard chemotherapy (cisplatin/pemetrexed) and immunotherapy treatments; (3) assess predictability of our 3D platform system in guiding personalized medicine approaches for mesothelioma by comparing patients-specific chemotherapy responses to *ex vivo* culture experiments. Through investigation of these goals, we found that in treatment naïve mesothelioma specimens, evaluation of pre-analytical variables demonstrated that prolonged ischemic times are associated with decreased tissue viability, lower tumor content, and decreased generation of spheroids. Treated specimens are consistently associated with low tissue viability, regardless of ischemic times. Separately, short-term analysis of drug therapies led to the treatment of mesothelioma samples with standard chemotherapy, revealing significant responses to this regimen in 3 of 5 samples. Experimental treatment with immunotherapy was also analyzed in one sample, however the response was not statistically significant ($p = 0.561$). Lastly, comparison of *ex vivo* and *in vivo* treatment responses demonstrated that 4 of 5 samples treated with standard chemotherapy had concordant responses to those of patients who received the same or similar post-operative therapy. As evaluated by our first aim, these data highlight the importance of streamlining human tissue collection and optimizing variables affecting the formation of PDOTS prior to *ex vivo* treatment analysis. Moreover, per our findings to aims two and three, the concordance observed in 3D cell culture and *in vivo* patient responses demonstrate the potential of this system to serve as predictive platform guiding future efforts in precision medicine.

Chapter 1: Introduction

I. Overview

II. Clinical Presentation and Assessment of MPM

Epidemiology and Presentation
Diagnostic Evaluation and Histologic Classification

III. Therapeutic Approaches

Chemotherapy
Surgery
Radiation

IV. Role of Precision Medicine in MPM

V. 3D Microfluidic Culture of Organotypic Tumor Spheroids

VI. Experimental Design

Chapter 1: Introduction

I. Overview

The mesothelium is a membrane comprised of simple squamous epithelial cells that line various serous cavities, including the pleura, peritoneum, pericardium and tunica vaginalis. Malignant transformation of these cells results in mesothelioma—a highly aggressive tumor with poor survival. Since more than 75% of cases arise in the pleura, malignant pleural mesothelioma (MPM) is the most common mesothelial cancer[1]**.** Unfortunately, treatment of this disease has proven challenging to address over the years. Curative methods have been attempted through the use of trimodality therapy (TMT) consisting of neoadjuvant and adjuvant chemotherapy, surgery, and radiation[2,3]. However, administration of neoadjuvant chemotherapy followed by surgical resection has shown that tumor recurrence is still common and prognosis remains poor with median survival at less than 29 months[4,5]. Given the fatal nature of this disease and limited effectiveness of conventional therapies, it is essential that novel approaches to treatment be considered.

II. Clinical Evaluation and Assessment of MPM

Epidemiology and Presentation

In the United States, the incidence of mesothelioma is estimated to be approximately 3300 cases per year[6]. Cases of early stage mesothelioma are associated with a 5-year survival of 15%, while those with late stage disease have a 5-year survival of less than 1%[7].The most important risk factor for this disease is inhalational exposure to asbestos, accounting for approximately 70% of pleural mesothelioma cases[8]. As a low-cost mineral made of magnesium silicate fibers, asbestos is valued for its insulation capacity making it widely used in construction, shipbuilding, and automotive industries. In the last 30 years, strict restrictions on asbestos exposure has led to a substantial reduction in disease incidence within the United States[9]. Generally, more industrialized countries have prioritized efforts to control asbestos utilization, banning importation, processing, and sale of this product. However, this is not the case in resource-limited countries. Worldwide incidence rates are still expected to climb in areas with poor regulation of asbestos and where usage of this

material is common[1]. Other causes of mesothelioma have been attributed to environmental, non-occupational asbestos exposure[10-11], ionizing radiation to supradiaphragmatic fields[12], genetic changes involving inactivation of the BRCA1-associated protein 1 (*BAP1)* gene[13-14] and, more controversially, exposure to simian virus 40 (SV40)[15].

The majority of patients diagnosed with MPM are older than 60 years of age and about 80% are men[16]. Since the disease is associated with a latency period of 10-50 years from time of exposure, patients often present with gradual onset of non-specific symptoms. These symptoms frequently include dyspnea, chest pain, cough, night sweats, and weight loss[16]. Invasion of local structures is rare but may present with more specific complaints. In addition, at the time of diagnosis almost all patients present with a pleural effusion. Common findings on physical exam include unilateral dullness to percussion at the affected lung base, decreased air movement, and restricted chest wall expansion. Overall, the insidious nature of this tumor coupled with non-specific findings on presentation, make knowledge of a patient's risk factors and health history paramount.

Diagnostic Evaluation and Biologic Classification

Evaluation of patients suspected of having MPM is initiated with imaging studies, including a chest x-ray and contrast-enhanced computed tomography (CT). More advanced imaging is typically performed using position emission tomography (PET) to assess for extent of disease. If a pleural effusion is present, thoracentesis is also routinely performed for cytologic evaluation of pleural fluid. However, pleural tissue is the best diagnostic source for confirmation of disease; to assess this directly, a closed pleural biopsy is completed. In the past, studies have shown that thoracentesis and cytologic evaluation of pleural fluid provides a diagnosis in 26% of cases compared to thoracentesis plus closed pleural biopsy where the diagnostic yield is 39%[17]. Consequently, in cases when closed pleural biopsies are unable to provide sufficient tissue or a definitive diagnosis, surgical intervention with video-assisted thoracoscopic (VATS) biopsy or open thoracotomy can be pursued. VATS has been shown to be diagnostic in up to 98% of cases[17]. Lastly, while there are no isolated biomarkers that can be used to confirm presence of disease, soluble mesothelin-related peptide (SMRP) is viewed as a promising marker. SMRP is overexpressed by mesothelin cells in MPM and can

be detected in peripheral blood and pleural effusions[18-20]. Since serum levels of SMRP can be significantly elevated in MPM, evaluation of this marker has been approved by the U.S. Food and Drug Administration for inclusion in disease diagnosis and monitoring[21].

During diagnosis of biopsied specimens, mesothelioma is broadly classified into three histologic subtypes: epithelioid, sarcomatoid, and biphasic (a mixed variant). Epithelioid tissue may include tubulopapillary, acinar, adenomatoid, and solid epithelioid patterns that often mimic non-neoplastic reactive mesothelioma cells[22]; about 60% of cases are diagnosed with this histology[23]. Contrastingly, sarcomatoid tissue consists of spindle cells in non-uniform bundles that often mimic malignant mesenchymal tumors; this variant accounts for 10-20% of cases. Biphasic or mixed mesotheliomas have features of epithelioid and sarcomatoid tumors. Understanding tissue histology not only aids in disease diagnosis, but also influences prognostic outcomes now that epithelioid tumor variants are associated with better overall survival compared to those with sarcomatoid or biphasic features[24-26].

III. Therapeutic Approaches

Chemotherapy

Treatment of malignant mesothelioma requires a multidisciplinary approach. Presently, standard therapy involves chemotherapy with pemetrexed coupled with a platinum compound (cisplatin or carboplatin)[27]. Pemetrexed is chemically similar to folic acid and acts as a folate antimetabolite to inhibit the formation of purine and pyrimidine precursors in DNA and RNA synthesis. Platinum compounds generally function by inhibiting DNA synthesis through the formation of DNA cross-links, denaturation of the double helix, and interference of DNA repair mechanisms[28]. The EMPHACIS trial helped show that median survival was significantly longer for patients who received the combination of cisplatin and pemetrexed versus cisplatin alone. Specifically, patients who received the combination therapy had a median survival of 12.1 months compared to 9.3 months for those who only received cisplatin[29].

Surgery

Beyond treatment with chemotherapy, patients with resectable disease often undergo surgery aimed at macroscopic complete resection (MCR) of the tumor[27]. For an operative approach to be considered in treatment, tumor spread is normally contained to one hemithorax and the patient has no contraindication to surgery. Two common operative approaches include complete lung removal via extrapleural pneumonectomy (EPP) versus lung sparing pleurectomy and decortication (P/D)[27]. Specifically, EPP is an *en bloc* resection of the parietal and visceral pleura that also removes the ipsilateral lung, pericardium, and diaphragm. In comparison, P/D involves removal of the parietal and visceral pleura to remove all gross tumor; the lung is left intact. Several recent studies have demonstrated decreased mortality, morbidity, and comparable overall survival with P/D compared to EPP[30-32].

Radiation

Briefly, the role of radiotherapy (RT) in MPM has changed over the years as techniques for radiation have improved and surgical approaches have changed. In the past, adjuvant treatment was given via external beam RT—a two-dimensional (anterior-posterior) approach that targeted the entirety of the affected hemithorax. This technique required blocking of unaffected organs (heart, kidneys, stomach) which often led to under dosing near blocked regions and increased risk of local failure[33]. With improved techniques, the use of adjuvant intensity-modulated radiation therapy (IMRT) became more common. This approach allowed for increased precision of tumor targets and more effective sparing of normal tissues. Several studies have demonstrated encouraging survival rates in patients who receive radiotherapy following surgery[34-36]. However, attempts to deliver tumoricidal doses of radiation to the pleura has raised concern for toxicity to the contralateral lung, often leading to fatal pneumonitis[37-38]. As the quest to improve RT continues, so do efforts to optimize this treatment modality in MPM.

IV. Role of Precision Medicine in MPM

Despite changes to surgical and radiation approaches, outcomes with trimodality therapy are variable and recurrence is commonly unavoidable[39]. Consequently, focusing on methods that can garner further success is necesary. Surgery and radiation have anatomical limitations to their curative potential; however, drug therapy approaches have not been fully explored. For the last 15 years, standard chemotherapy for this disease has been a combination of cisplatin and pemetrexed[29]. While this combination is known to prolong patient survival, the patient response rate to these agents is about 30%[40]. This provides room for further investigation of patient-specific susceptibility to cancer therapy.

Today, poor response to anti-cancer drugs is an important challenge in clinical oncology. Limited or resistant cancers can in part be attributed to tumor heterogeneity, gene amplification, DNA-damage repair, drug inactivation, epithelial-mesenchymal transition (EMT), and epigenetics[41]. Despite intrinsic patient and tumor variability to drugs, for years decisions guiding novel therapies have been made based on population-specific rather than patient-specific treatment responses. Personalized medicine has surfaced as a way to tailor cancer therapies for patients[42]. Given the complex interactions between cancer cells and the immune system, it is important that platforms studying precise therapies can recapitulate cellular exchanges unique to the patient-tumor microenvironment (TME). One such platform involves microfluidics using patient-derived organotypic spheroids (PDOTS)[43].

V. 3D Microfluidic Culture of Organotypic Tumor Spheroids

As more focus is given to personalized cancer therapy approaches, there is a critical need to develop *ex vivo* systems that can recapitulate biological interactions intrinsic to the tumor microenvironment. To be effective, these systems need to mimic the continuous interactions that exist between tumor cells and non-tumor components. Since three-dimensional (3D) culture systems have the advantage of replicating the complex microcosm in which tumor, stromal, and immune cells are imbedded, they proffer an advantage over conventional macroscopic cell culture models[44-45]. Recently, we demonstrated successful *ex vivo* growth of organotypic tumor spheroids in syngeneic murine models and patient tumors[43]. Spheroids in this study were analyzed using the DAX-1 3D cell culture chip from AIM Biotech[46].

Combination of 3D culture with microfluidics provides an enhanced platform via which tumor spheroids can be characterized and analyzed using different techniques, including cytokine profiling, RNA sequencing, live-dead analysis, and immunofluorescence[43,47].

While other methods to study cancer therapies include the use of organoids[48-49], patient-derived xenografts (PDXs)[50], and circulating-tumor cells (CTCs)[51], the use of PDOTS also provides the unique advantage of rapid drug screen capabilities bypassing days or weeks of tissue manipulation needed for organoid and PDX production. Having a platform with rapid drug analysis potential allows for exploration of new therapeutic elements (i.e. immune checkpoint inhibitors, ICI) and their combination with conventional treatment. In light of these advantages, we generated mesothelioma organotypic spheroids and used them in conjunction with microfluidic culture for the investigation of novel therapies.

VI. Experimental Design

Experiments in this study were designed to investigate new therapeutic regimens in mesothelioma via 3D culture models of patient-derived organotypic spheroids. The goals of this study encompassed three research aims. First, we sought to optimize tumor tissue characterization and allocation practices in this tumor. Presently, no formal studies have evaluated variables that may impact tumor content and cell viability in mesothelioma. Consequently, pre-analytical variables predicted to possibly affect successful generation of spheroids were assessed from the operating room to the lab bench. These variables included: neoadjuvant chemotherapy administration, pleurodesis status, type of surgery, tissue fibrosis, and tissue ischemia times. Secondly, short term comparative analysis of tumor responses to standard chemotherapy versus novel combination treatments using immunotherapy approaches was performed. Live-dead cell analysis was utilized to determine tumor responses to drug testing. Lastly, the predictability of our 3D platform system was evaluated by comparing *in vivo* patient-specific chemotherapy responses to *ex vivo* culture experiments.

Chapter 2: Materials and Methods

I. Patient Samples
Specimen appropriation
Pre-analytical variable tracking

II. Spheroid Preparation and Microfluidic Culture
Generation of patient-derived organotypic tumor spheroids (PDOTS)
Ex vivo treatment combination

III. Microfluidic Device Design

IV. Immunofluorescence Analysis
Indirect immunofluorescence and antibodies
Imaging

V. Live/Dead Staining
Immunofluorescence and antibodies
Imaging
Quantification

VI. Statistical Methods

I. Patient Samples

Specimen Appropriation

A cohort of patients treated at Brigham and Women's Hospital (BWH) and Dana-Farber Cancer Institute (DFCI) was assembled for PDOTS profiling and culture between November 2017 and April 2018. Tumor samples were collected from consented patients included in the pre-approved Molecular Markers in Human Tissue IRB Protocol #98-063.

Pre-Analytical Variable Tracking

Pre-analytical variables potentially impacting generation of patient-derived spheroids were collected for the majority of tissue specimens. Variables studied included: administration of neoadjuvant chemotherapy, pleurodesis status, type of surgery, presence of fibrosis, and onset of warm and cold ischemia during tissue retrieval and processing. Patient data for neoadjuvant chemotherapy and pleurodesis status was obtained from patient charts accessed by clinical research assistants (CRAs) and blind to all researchers. Data was provided to our lab in a de-identified fashion. On the day of surgery, type of surgery, tissue ischemia time, and extent of specimen fibrosis was recorded. Onset of warm ischemia was defined as the time from which a pleural specimen was removed from the lung or time the pulmonary artery was clamped during surgery. Onset of cold ischemia was defined as the time at which pleural specimen was placed in in media and on ice.

A schematic representation of tissue processing from the operating room to the lab bench is summarized in Figure 1.

II. Spheroid Preparation and Microfluidic Culture

Generation of Patient-derived organotypic tumor spheroids (PDOTS)

Preparation of PDOTS was performed as previously described[43] and is illustrated in the workflow schematic of Figure 2. Briefly, fresh tumor tissue was received in media (DMEM or RPMI) on ice and minced in a standard 10cm dish using sterile forceps and scalpel. Minced tumor was suspended in DMEM (4.5 mmol/L glucose, 100 mmol/L Na pyruvate, 1:100 penicillin–streptomycin; Corning CellGro) + 10%FBS, 100 U/mL collagenase type I,

and 15mmol/L HEPES. Samples were pelleted and resuspended in fresh DMEM + 10% FBS and subsequently strained over a 100μM and 40μM filter. This filtering process produced three fractions of spheroids: S1 spheroids (>100μM), S2 spheroids (40-100μM) and S3 spheroids (<40μM). Since increased spheroid size can lead to cell hypoxia[52] spheroids >100μM were not utilized. S2 fractions were utilized for *ex vivo* culture and maintained in ultralow-attachment tissue culture plates. An aliquot of the S2 fraction was then pelleted and resuspended in type I rat tail collagen (Corning) at a concentration of 2.5 mg/mL with addition of 10% PBS with phenol red adjusted to pH 7.0-7.5 using NaOH and confirmed with Panpeha Whatman paper (Sigma-Aldrich). The spheroid-collagen mixture was subsequently injected into the 3D microfluidic cell culture device (AIM Biotech). Devices with spheroid-collagen suspension were placed in a sterile humidity chamber and incubated for 30 minutes at 37°C. Post incubation, the collagen hydrogel containing PDOTS was hydrated with fresh media (DMEM or RPMI) and underwent further characterization or treatment.

Ex vivo treatment combinations

Following generation of PDOTS and incubation of the collagen-spheroid mixture (as described above), media with standard and experimental therapeutic regimens for MPM was added to microfluidic devices. PDOTS were treated with standard agents pemetrexed (1uM – 4uM) and cisplatin (1.5uM – 20uM). Experimental immunotherapy treatments included anti-PD-1 (pembrolizumab, 250 ug/mL) and anti-CTLA-4 (ipilimumab, 50ug/mL). Once treatments were added to microfluidic devices, they were incubated in a sterile humidity chamber for 4-6 days at 37°C.

III. Microfluidic Device Design

Microfluidic cell culture devices used in this study are described extensively by Farahat et al.[53] and Amir et al.[46]. Succinctly, devices consist of a central channel region responsible for caging the collagen solution. On either side of this region are two media channels that run in parallel and feed directly into the central channel. Devices are formed by bonding a coverslip to a patterned polydimethylsiloxane (PDMS) substrate. Cell responses can be tested by modifying the composition of growth media in the channels or introducing therapeutic

agents. Spheroid and single cell behavior can be observed via 3D confocal imaging of the various channels through the supporting glass coverslip.

IV. Immunofluorescence Analysis

Immunofluorescence and antibodies

Characterization of spheroids was performed via 4-color immunofluorescence. PDOTS were washed with PBS and blocked with Fc receptor (FcR) blocking reagent (Miltenvi) for 15 minutes at room temperature. Directly-conjugated antibodies were used for the following human markers: CD45, CD8, CD11b, CD90 , and PD-L1. Antibodies were diluted 1:50 in 10ug/mL solution of Hoechst 33342 (Thermo Fisher Scientific) in PBS and added to media wells in microfluidic devices for 45 minutes at room temperature in the dark. PDOTS were washed twice using PBS with 0.1% Tween20 followed by PBS alone. To assess viability, a 1:1000 solution of calcein AM (Thermo Fisher Scientific) in PBS was loaded into the microfluidic devices and incubated for 5 minutes at room temperature in the dark. Following this incubation, imaging was performed.

Imaging

Images of single cells and spheroids in culture were obtained using a Nikon Eclipse 80i fluorescence microscope equipped with Z-stack (Prior) and CoolSNAP CCD camera (Roper Scientific). Capture of images and further analysis was done using the NIS-Elements AR software package.

V. Live/Dead Staining

Immunofluorescence

Live-dead fluorescence was performed by loading microfluidic devices with Nexcelom ViaStain AO/PI Staining Solution (Nexcelom, CS2-0106) or through the use of Hoechst/propidium iodide. When using the ViaStain AO/PI Staining Solution, devices were incubated for 20 minutes at room temperature in the dark. Separately, when using Hoechst/priopidium iodide, devices were incubated with dyes for 40 minutes at 37°C.

Imaging

As previously noted, images were captured on a Nikon Eclipse 80i fluorescence microscope equipped with Z-stack (Prior) and CoolSNAP CCD camera (Roper Scientific). Capture of images and further analysis was done using the NIS-Elements AR software package. Image deconvolution was performed with AutoQuant Module and whole device images were achieved by stitching multiple captures.

Quantification

Cell quantitation was done by measuring total cell area of each dye, ultimately capturing total cell area of dead cells and total cell area of live cells.

VI. Statistical Methods

Statistical analysis were performed in GraphPad Prism version 8 (La Jolla, CA) and R version 3.4.1 (Vienna, Austria) statistical package[54]. Student's T test and Fisher's Exact tests were performed to evaluate demographic variables. A student's T test was also used to analyze live/dead cell responses between experimental and control groups. All graphs (Figures 4-8) depict mean SD unless otherwise indicated.

.

Chapter 3: Results

I. Optimization of PDOTS generation from mesothelioma specimens

Tissue processing and allocation
Evaluation of pre-analytical variables from the OR to the lab bench

II. Microfluidic culture in mesothelial PDOTS

Characteristics of mesothelioma specimens selected for treatment analysis
Mesothelioma specimen 5: Immune profiling and *ex vivo* culture of standard therapy
Mesothelioma specimen 7: Immune profiling and *ex vivo* culture of standard therapy
Mesothelioma specimen 15: Immune profiling and *ex vivo* culture of standard therapy
Mesothelioma specimen 16: Immune profiling and *ex vivo* culture of standard therapy
Mesothelioma specimen 14: Immune profiling and ex vivo culture of immunotherapy

III. Evaluation of *ex vivo* and *in vivo* treatment responses in MPM

I. Optimization of PDOTS generation from mesothelioma specimens

Tissue processing and allocation

To evaluate quality of mesothelioma tumor specimens, steps in tissue processing and allocation were carefully observed. All mesothelioma samples were collected during surgery prior to being analyzed by pathology for gross estimates of tumor content, histology verification, and allocation to research. During this process, steps taken for tissue collection in the operating room and subsequent processing in pathology were not always uniform and often led to variations in tissue handling, placement of samples in media, and conservation on ice. These differences in specimen collection coupled with variability in tissue viability and tumor content during spheroid analysis led to a streamlined approach in observation of pre-analytical variables (Figure 1) prior to generation of PDOTS (Figure 2).

Evaluation of pre-analytical variables from the OR to the lab bench

To assess successful generation of PDOTS, five variables were investigated during tissue processing: neoadjuvant chemotherapy status, pleurodesis status, type of surgery, presence of fibrosis and interval between warm and cold ischemia. Although 31 mesothelioma samples were processed during this study, pre-analytical variable data was collected for 23 pleural specimens. Within this cohort, assessment of tissue ischemia and cell viability was done based on treatment status with neoadjuvant chemotherapy. In treatment naïve specimens (n=9), the average tissue ischemia time was 28 minutes (range 10-56 minutes). Within this group, it was generally observed that prolonged ischemic times were associated with decreased tissue viability (Table 2A). Extended ischemia was also associated with lower tumor yield and decreased generation of spheroids. In pleural specimens exposed to neoadjuvant chemotherapy, the average tissue ischemia time was 66 minutes (range 29-195 minutes). With the exception of mesothelioma sample #11, these samples were consistently associated with low tissue viability ($\leq$ 30% live cells) irrespective of ischemic time (Table 2B). In addition, there was increased tumor fibrosis (data not shown) and tumor content was non-analyzable in most samples. Mesothelioma sample #11 was notable in that its viability and tumor content were high at 75% and 85%, respectively, despite being exposed to neoadjuvant chemotherapy. Lastly, a subset of mesothelioma specimens were found to have

low viability (< 30% live cells) despite treatment naïve status and low ischemic times (average ischemia was 34 minutes; range 16-72 minutes) (Table 2C). Overall, these specimens were more likely to have biphasic tumor histology (4 of 5 samples).

II. Microfluidic culture in mesothelial PDOTS

Characteristics of mesothelioma specimens selected for treatment analysis

A total of 31 pleural specimens were processed during the time of this study. Initial evaluation of sample viability was done with Nexcelom ViaStain AO/PI staining solution on S3 fraction. Samples with viability greater than 15% were processed further via 4-color immunofluorescence. In this setting, viability was determined by calcein AM/DRAQ7 or PI staining. Tumor content was also analyzed via IF. To date, there is no common marker for detection and confirmation of mesothelioma tumor cells. However, many tumors with epithelioid histology may express CD90[55]. Unfortunately, the expression of this marker is not universal and can be absent in biphasic and sarcomatoid tumors. Consequently, we defined tumor content by the absence of the general immune marker, CD45. Specimens with immunofluorescence revealing tumor content greater than 50% and more than 20 spheroids per well were selected to investigate responses of PDOTS to standard chemotherapy and immunotherapy (Figure 3). Notably, for the assessment of immunotherapy responses, information about immune status of tumor is important. Hence, during IF analysis we recorded the presence of CD8 T-cells and PD-L1 expression in tumor cells.

For all study components between samples that were treated (n=10) and untreated (n=21), no significant differences were appreciated in age, gender, medical history (history of asbestos exposure and smoking), administration of neoadjuvant chemotherapy, type of surgery, and tissue histology. Although not statistically significant (p=0.055), treated specimens were generally less likely to have been exposed to neoadjuvant chemotherapy (Table 1). Ultimately, four representative samples of the treated cohort were selected to discuss immune profiling and *ex vivo* culture with standard chemotherapy and one sample was selected to discuss immunotherapy responses.

Mesothelioma specimen 5: Immune profiling and ex vivo culture of standard chemotherapy

Specimen 5 was a treatment naïve sample found to have a biphasic histology with predominant sarcomatoid features. Immunofluorescence revealed 50% cell viability, 60% tumor content, 20% CD90+ cells, and 60 CD8 T cells per well. Live cells can be appreciated with calcein AM whereas dead cells are visualized with DRAQ7 staining (Figure 4A). In addition, some single CD8 T-cells are visible following IF with anti-CD8 monoclonal antibody (Figure 4A). Percent live/dead analysis of PDOTS treated with cisplatin (1.5uM) and pemetrexed (1uM) versus media control revealed no statistically significant difference ($p = 0.294$) between these groups (Figure 4B).

Mesothelioma specimen 7: Immune profiling and ex vivo culture of standard chemotherapy

Specimen 7 was a treatment naïve sample found to have epithelioid histology. Immunofluorescence revealed 60% cell viability, 50% tumor content, 10% CD90+ cells, and 50 CD8 T-cells per well. Immune cells can be appreciated with anti-CD45 monoclonal antibody and CD90+ cells with anti-CD90 monoclonal antibody (Figure 5A). In addition, some cells were found to be faintly positive for PD-L1 (Figure 5A). Percent live/dead analysis of PDOTS treated with cisplatin (1.5uM) and pemetrexed (1uM) versus media control revealed a statistically significant difference ($p = 0.002$) between these groups (Figure 5B).

Mesothelioma specimen 15: Immune profiling and ex vivo culture of standard chemotherapy

Specimen 15 was a treatment naïve sample found to have a biphasic histology with predominant epithelioid features. Immunofluorescence revealed 30% cell viability, 50% tumor content, and low CD8 count (0-5 CD8 per well). Given prior resistant responses of some tumors to standard chemotherapy, this tumor was treated with pemetrexed (1uM) and cisplatin at two different concentrations (2uM and 20uM). Percent live/dead analysis of PDOTS treated with cisplatin and pemetrexed versus media control revealed a statistically

significant difference at p = 0.028 for combination treatment with cisplatin 2uM and p = 0.017 for combination treatment with cisplatin 20uM (Figure 6).

Mesothelioma specimen 16: Immune profiling and ex vivo culture of standard chemotherapy

Specimen 16 was a treatment naïve sample found to have a biphasic histology with predominant epithelioid features. Immunofluorescence revealed 80% cell viability, 90% tumor content, 10% PD-L1+ cells, and low CD8 count (0-5 CD8 per well). CD45 and CD8 immune cells can be appreciated with anti-CD45 and anti-CD8 monoclonal antibodies (Figure 7A-B). In addition, live cells can be appreciated with calcein AM (Figure 7B). Given prior resistant responses of some tumors to standard chemotherapy, this tumor was treated with pemetrexed (1uM) and cisplatin at two different concentrations (2.5uM and 20uM). Percent live/dead analysis of PDOTS treated with cisplatin and pemetrexed versus media control revealed no statistically significant difference at p = 0.508 for combination treatment with cisplatin 2.5uM and p = 0.073 for combination treatment with cisplatin 20uM (Figure 7C).

Mesothelioma specimen 14: Immune profiling and ex vivo culture of standard chemotherapy and immunotherapy

Specimen 14 was a treatment naïve sample found to have an epithelioid histology. Immunofluorescence revealed 50% cell viability, 90% tumor content, CD90 negative cells, PD-L1 negative cells, and 30 CD8 T-cells per well. Immune cells can be appreciated with anti-CD45 monoclonal antibody and live cells with calcein AM (Figure 8A). This tumor was treated with immunotherapy (anti-CTLA-4 at 50ug/ml and anti-PD-1 at 250ug/ml) and standard chemotherapy (pemetrexed at 1uM and cisplatin 1uM). When compared to the media control, there was no statistically significant difference for percent live/dead cells treated with immunotherapy (p = 0.561) but there was a significant difference for those treated with standard chemotherapy (p = 0.015) (Figure 8B).

III. Evaluation of *ex vivo* and *in vivo* treatment responses in MPM

Since the analysis of all mesothelioma specimens for this study, several patients diagnosed with MPM have been treated with adjuvant or salvage chemotherapy. Adjuvant and salvage chemotherapy are often a combination of cisplatin and pemetrexed with or without bevacizumab (a vascular endothelial growth factor (VEGF) inhibitor that has shown to be advantageous in some studies for the treatment of MPM[56]). After treatment with these therapies, patients are followed closely to monitor tumor status via routine radiographic assessments. In an effort to evaluate the predictability of our 3D microfluidic model, responses of PDOTS treated with standard chemotherapy *ex vivo* were compared to the most recent radiographic response of patients who received adjuvant or salvage chemotherapy. These responses were assessed for patients with tumor tissue that corresponded to mesothelioma specimens 5, 7, 15, 16, and 14 (Figures 4-8).

From the mesothelioma specimens treated with standard chemotherapy, four of five samples had *ex vivo* treatment responses that were concordant to patient responses (Figures 4-8). PDOTS for mesothelioma specimens 7, 14, and 15 all responded to standard treatment *ex vivo* as did patients who received adjuvant chemotherapy with similar agents (Figure 5, 6, and 8). PDOTS for mesothelioma specimen 5 did not respond to standard treatment *ex vivo* nor did the patient following treatment with salvage therapy (Figure 4). Lastly, while PDOTS for mesothelioma specimen 16 did not respond to standard chemotherapy, the patient affiliated with this tumor has not had a recurrence to date following adjuvant chemotherapy (Figure 7).

Chapter 4: Discussion

Malignant pleural mesothelioma is a highly aggressive tumor with limited curative therapies. Treatment with cisplatin/pemetrexed has resulted in an increase of overall survival by 3 months[29] while recent addition of bevacizumab has garnered an additional benefit of a similar 3-month period[56]. However, no other therapies have shown improvement in randomized controlled trials and attempts at a multimodal approach to treatment have not been successful. Consequently, considering novel treatment methodologies for this fatal disease is essential.

In oncology, the use of precision medicine involves identifying genomic alterations or distinct tumor characteristics that can be used to target specific therapies to individual patients. This approach to cancer treatment is well-poised to be integrated into routine clinical decision-making[57, 58]. However, the inability to confirm whether a correlation exists between genetic alterations or individualized tumor features and response to therapeutic agents has limited the number of patients who can potentially use precision medicine therapy. Presently, only 11% of patients tested for discrete genetic changes in solid tumors go on to follow precision medicine guided treatments[59]. Beyond gene-targeting therapies, this challenge also applies to understanding the predictive capacity of patient responses to immunotherapy and, more broadly, chemotherapy[43]. With efforts focused on comprehension of drug predictability in cancer, adequately investigating tumor tissue specimens as representatives of a more complex pathologic process is beneficial.

To date, various systems have been used to study patient tumor specimens. One such model includes the use of 2D cell culture for the evaluation of tumor cell lines. While this approach is inexpensive, well-established, and allows for easy manipulation of cell lines, the planar distribution of cells do not accurately recapitulate the 3D microenvironment of tumors *in vivo*[60]. Moreover, doses of drugs found to be of benefit in 2D culture are not commonly effective when given to patients[61,62]. Hence, growth of tumor cells in 3D, especially in the presence of stromal and immune components allow better replication of *in vivo* effects and more accurate design to evaluate cancer cell responces[43].

In this study, we used microfluidic 3D culture to investigate short-term *ex vivo* responses of mesothelioma spheroids to standard and experimental therapies. However, before being able to conduct this analysis, it was fundamental to optimize generation of PDOTS in mesothelioma. To this end, we evaluated several pre-analytical variables in 23 tumor specimens from time of collection in the operating room to time of analysis in the lab; namely, these included neoadjuvant chemotherapy administration, pleurodesis status, type of surgery, tissue fibrosis, and tissue ischemia times. From the samples assessed, three groups were created based on exposure to neoadjuvant status. In treatment naïve samples, it was generally observed that prolonged ischemic times were associated with decreased tumor viability, tumor content, and generation of spheroids (Table 2A). Yet, samples previously treated with neoadjuvant chemotherapy were consistently associated with low tissue viability, irrespective of ischemic time (Table 2B). This difference is possibly attributed to augmentation of cell death during the administration of neoadjuvant chemotherapy, predisposing tumor tissue to an increased presence of acellular material. In fact, many of the treated samples were often found to have a larger proportion of fibrotic material compared to treatment naïve specimens. An exception to this response was mesothelioma sample 11 which was found to have high viability (75% live cells), possibly due to tumor resistance leading to a very limited response to primary chemotherapy. Conversely, a subset of mesothelioma specimens was found to have low viability despite treatment naïve status and short ischemic times (Table 2C), indicating there may be other factors impacting tissue quality. For this subset, all samples had a biphasic histology comprised of epithelioid and sarcomatoid features. Given the presence of a sarcomatoid landscape, it is important to consider the behavior of this cell type. In particular, sarcomatoid cells are known to have quick, sporadic growth patterns that are detrimental to patient prognosis. Their spindle shape often makes it hard to differentiate from other tumors and fibrotic tissue. Macroscopically, the tissue is firm and rubbery while microscopically it can have spindled, irregular, and fibrous features making it difficult to distinguish from other mesenchymal tumors, pleural plaques, and fibrous pleuritis, even after immunohistochemistry analysis[63]. Consequently, variability in percent of live cells within this smaller cohort may possibly reflect the irregular nature of this histologic type. Beyond histology, another factor to consider includes pleurodesis status—a procedure used for patients with recurrent pleural effusions aimed at obliterating the pleural space frequently causing fibrosis of this tissue. Lastly, intrinsic tumor heterogeneity can also contribute to the

differences observed. These data ultimately highlight the challenges associated with performing studies on human materials and emphasize how streamlining processes for tissue collection can optimize success of *ex vivo* cancer models in guiding functional precision therapies.

With better understanding of factors that may impact tumor tissue quality in mesothelioma, generation of spheroids improved during the trajectory of this study. Many of the treatment naïve samples, which generally had higher tumor content and cell viability, contributed to the subsequent evaluation of short-term therapy responses of mesothelioma spheroids in 3D microfluidic culture**.** In particular, a total of 10 samples underwent treatment in *ex vivo* culture with no significant demographic differences in age, gender, medical history, neoadjuvant chemotherapy administration, surgery type, and histology between treated and untreated groups (Table 1).

The treatment modalities tested included standard chemotherapy with cisplatin and pemetrexed combined and immunotherapy with ipilimumab (anti-CTLA-4) and pembrolizumab (anti-PD-1) combined. From all treated specimens, five are reported as representative samples from the total cohort. Complete *ex vivo* and *in vivo* response data was available for these specimens allowing for a full discussion of our findings. In samples receiving standard chemotherapy (mesothelioma specimens 5, 7, 14, 15, and 16) there was a predominance of epithelioid pathology (60%, Table 1) coinciding with the general histologic distribution observed in this tumor. Additionally, the viability was >30% and tumor content >50% in all cases (Figures 4 - 8) further strengthening the trends observed during tracking of pre-analytical variables. Immunofluorescence analysis revealed presence of CD90+ cells in two samples: mesothelioma 5 and 7 (Figure 4 and 5), respectively. Although the expression of this marker is inconsistent, it can be found in mesothelial tumors containing epithelioid features[55] which coincides with the pathologic findings of samples 5 and 7, further complementing the assessment of tumor content in these specimens. Lastly, with the intention of possibly testing immunotherapy as an experimental treatment in this study, all samples underwent assessment of CD8 count and PD-L1 during IF. Although a single sample (mesothelioma 16) demonstrated faint PD-L1 expression, samples 5, 7, and 14 were found to have high to moderate CD8 counts at 60, 50, and 30 cells per well, respectively. The

high number of CD8 T-cells in early samples helped support selection of immunotherapy as an experimental treatment for specimens obtained later in our study.

In this study, prior to assessing immunotherapy responses *ex vivo*, we analyzed tumor responses to standard chemotherapy. Of the five mesothelial samples discussed here, mesothelioma samples 7, 15, and 14 were found to have statistically significant responses to cisplatin/pemetrexed compared to the media control while samples 5 and 16 were resistant. These differences can potentially be attributed to tumor histology, heterogeneity, and limitations of *ex vivo* culture. For example, mesothelioma sample 5 is the only specimen with a predominant sarcomatoid histology, possibly predisposing it to more resistant tumor mechanisms given the aggressive nature of this pathology[64]. On the other hand, mesothelioma sample 16 was treated with combinations of pemetrexed (1uM) and cisplatin at different concentrations (Cisplatin 2.5uM and 20uM) to evaluate if there was a concentration-dependent tumor response. While treatment at lower concentration of cisplatin did not yield a significant response ($p = 0.508$) compared to the control, treatment at higher concentration brought a non-significant response to a more marginal level ($p = 0.073$).

Assessment of immunotherapy responses was performed understanding that immune checkpoint blockade (ICB) inhibitors have been an effective treatment modality in different cancers[65,66]. The ability to employ this therapeutic approach stems from understanding of tumor adaptation and upregulation of ligands inhibitory to tumor-infiltrating immune cells. Therapy involving ICB uses antibodies to block inhibitory signaling and activate immune cells. In MPM, there are several ongoing clinical trials evaluating checkpoint inhibition with antibodies against CTLA-4 and the PD-1/PD-L1 pathway[67]. Because of this, more studies have focused on evaluating the immune environment in mesothelial tissue[64] and assessing models that can be predictive of tumor responses against these agents.

In this study, response to immunotherapy (ipilimumab and pembrolizumab combined) was evaluated in sample 14. However, no statistical difference was found between this regimen and the control ($p = 0.561$). Although many factors can influence this response, these results could be attributed to the more moderate T-cell infiltration seen in this sample (CD8 = 30 cells/well).

Indeed, without a robust immune presence the effects of immunotherapy on this tumor can be quite limiting especially since mesothelioma tissue can be accompanied by a generally noninflamed state[68]. While these tumor characteristics can make mesothelioma more difficult to utilize within the context of immunotherapy, having a platform where its microenvironment can continue to be studied and tested for responses *ex vivo* is very important. In this way, if the tumor is found to be inflamed or if it is positive for certain immune checkpoint blockade markers (i.e. PD-L1), these findings can be used for designing and testing patient-specific treatments.

In the last phase of this study, we compared *ex vivo* culture responses to *in vivo* patient responses. Specifically, patient responses were provided in a de-identified fashion by clinical research assistants with access to radiographic assessments of patient tumor burden. Traditionally, imaging evaluations use the standards delineated by the response evaluation criteria in solid tumors (RECIST, Version 1.1)[69] to assess for disease progression. De-identified data addressed responses based on whether a recurrence occurred (progressive disease noted by radiology) or whether there was no recurrence to date (either stable disease or partial response noted by radiology). Unfortunately, a clear delineation between stable disease and partial response could not be provided for our samples. Per the RECIST criteria, progressive disease (PD) is defined as a 20% increase in the sum of diameters of target lesions with an absolute increase of at least 5mm from prior or one or more new lesions. Partial response (PR) is defined as a 30% decrease in the sum of diameters of target lesions. Finally, stable disease (SD) is described as having no sufficient increase in tumor burden to qualify as PD nor sufficient shrinkage to qualify as PR. Overall, 4 of 5 samples reported here were found to have concordant responses between *ex vivo* and *in vivo* settings (Figures 4, 5, 6, and 8). Mesothelioma specimens 5 was not responsive to treatment *ex vivo* ($p = 0.294$) and the patient *in vivo* was noted to have progressive disease following salvage therapy with carboplatin, pemetrexed and bevacizumab. While the patient did receive a more potent regimen with the addition of bevacizumab, it is valuable to note that the tumor specimen *ex vivo* did not respond even when the therapy modality lacked that drug. Thus, concordance to the lack of response was noted even with standard agents. Mesothelioma specimens 7, 14, and 16 all demonstrated strong responses to standard chemotherapy *ex vivo* and, in a similar fashion, all corresponding patients have not had a tumor recurrence to date. This was after patients received adjuvant chemotherapy with a combination of

a platinum agent (cisplatin or carboplatin) and pemetrexed. Lastly, mesothelioma specimen 16 demonstrated a discordant response between *ex vivo* and *in vivo* responses. In particular, this sample was tested at two different concentrations of cisplatin. While there was no significant response to either concentration, the difference between treatment with cisplatin/pemetrexed at a high dose was more pronounced ($p = 0.073$) than treatment at a lower cisplatin dose ($p = 0.508$). Notably, the standard deviation in the control had a wide distribution in this sample. If this distribution had been more tightly conserved, it is likely this specimen would have passed the criteria to be responsive to standard therapy.

Despite the benefits found in the analysis of mesothelioma PDOTS, there are several important limitations. First, a strong drawback of this study is its small sample size. While definite conclusions cannot be made regarding tissue evaluation and processing, tumor treatment responses, and correlations of 3D culture findings to *in vivo* responses, this work emphasizes the general trends within each of those areas. Second, given the limited samples for study, this investigation often explored several variables without always having these changes consistently applied to all specimens. For example, once we noted that some mesothelioma specimens benefitted from higher concentrations of cisplatin, different concentrations of this drug were utilized and applied to later samples, but are not seen in early samples. Similar exploration was taken with testing experimental treatments and their combinations. Third, comprehensive evaluation of all stromal and immune components was not feasible. While multicolor IF allowed us to differentiate between immune and tumor cell types and evaluate the number of cytotoxic T-cells, a more sensitive approach (i.e. flow cytometry or single-cell RNA-seq) would be beneficial to evaluate presence of other cell types. Fourth, spheroids within our 3D microfluidic device were not evaluated for metabolic parameters (hypoxia, glucose levels, etc.) which may impact cell responses to treatments tested. Ultimately, although this is a small cohort of samples with various limitations, concordance trends observed thus far show promise in the utilization of our PDOTS microfluidic cultures system to evaluate tumor responses *ex vivo*.

Overall, this work provides a foundation for future investigations evaluating mesothelioma specimens. Specifically, this is done within the context of a novel 3D microfluidic system that can better facilitate evaluation of patient-specific responses to different therapies. Future work

could benefit from further validation studies for this system. In particular, more experiments testing standard chemotherapy in mesothelioma specimens could increase the sample size and power of results discussed here. Moreover, additional experimental treatments can be considered for exploration and be conducted in a uniform manner. For example, preliminary testing of inhibitors against signal transducer and activator of transcription 3 (STAT 3)—known to be involved in cell proliferation, survival, angiogenesis, and tumor evasion among many other functions—demonstrated promising results in a small cohort of mesothelioma samples tested in our lab (data not shown). Lastly, future work could benefit from further understanding of the tumor microenvironment contexture through studies focused on cytokine profiling following treatment of specimens and further evaluation of immune component through flow cytometry and RNA sequencing.

Chapter 5: Summary

As more focus is given to personalized cancer therapy approaches, there is a critical need to develop *ex vivo* systems that can recapitulate biological interactions intrinsic to the tumor microenvironment. Consequently, this study focused on the utilization of patient-derived organotypic tumor spheroids for the exploration of precision medicine advances in malignant pleural mesothelioma. Through the initial aim of this research, we identified pre-analytical variables that were found to impact generation of spheroids in the lab. In particular, we noted that administration of neoadjuvant chemotherapy was an important factor impacting cell viability and tumor content. We also performed short-term analysis of tumor responses to standard chemotherapy and immunotherapy combinations. Based on the analysis of a small cohort of mesothelial samples, the impact of tumor heterogeneity, histology, and experimental variability were discussed as elements impacting tumor responses. Lastly, we evaluated the predictability of our 3D platform system by comparing patient-specific chemotherapy responses to *ex vivo* culture experiments, remarking on the predominant trend toward concordant responses between these settings. Thus, these early findings emphasize the utility of spheroids in modeling short-term responses to standard and experimental therapeutic regimens. Through future work, this system may provide an avenue to better understand and evaluate the complexities of tumor and drug interactions that guide so many of the current efforts in functional precision medicine.

Figures and Tables

I. **Figures**

II. **Tables**

III. **Legends**

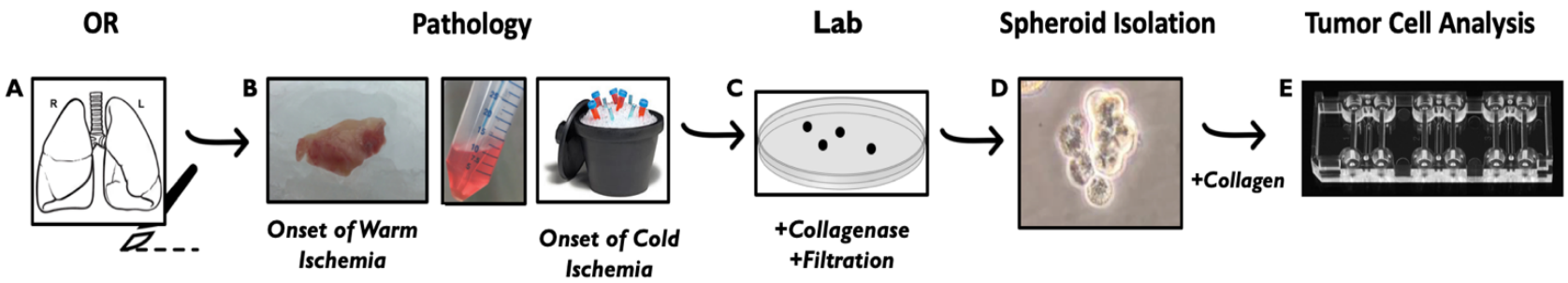

Figure 1. Tissue processing from the operating room to the lab bench.

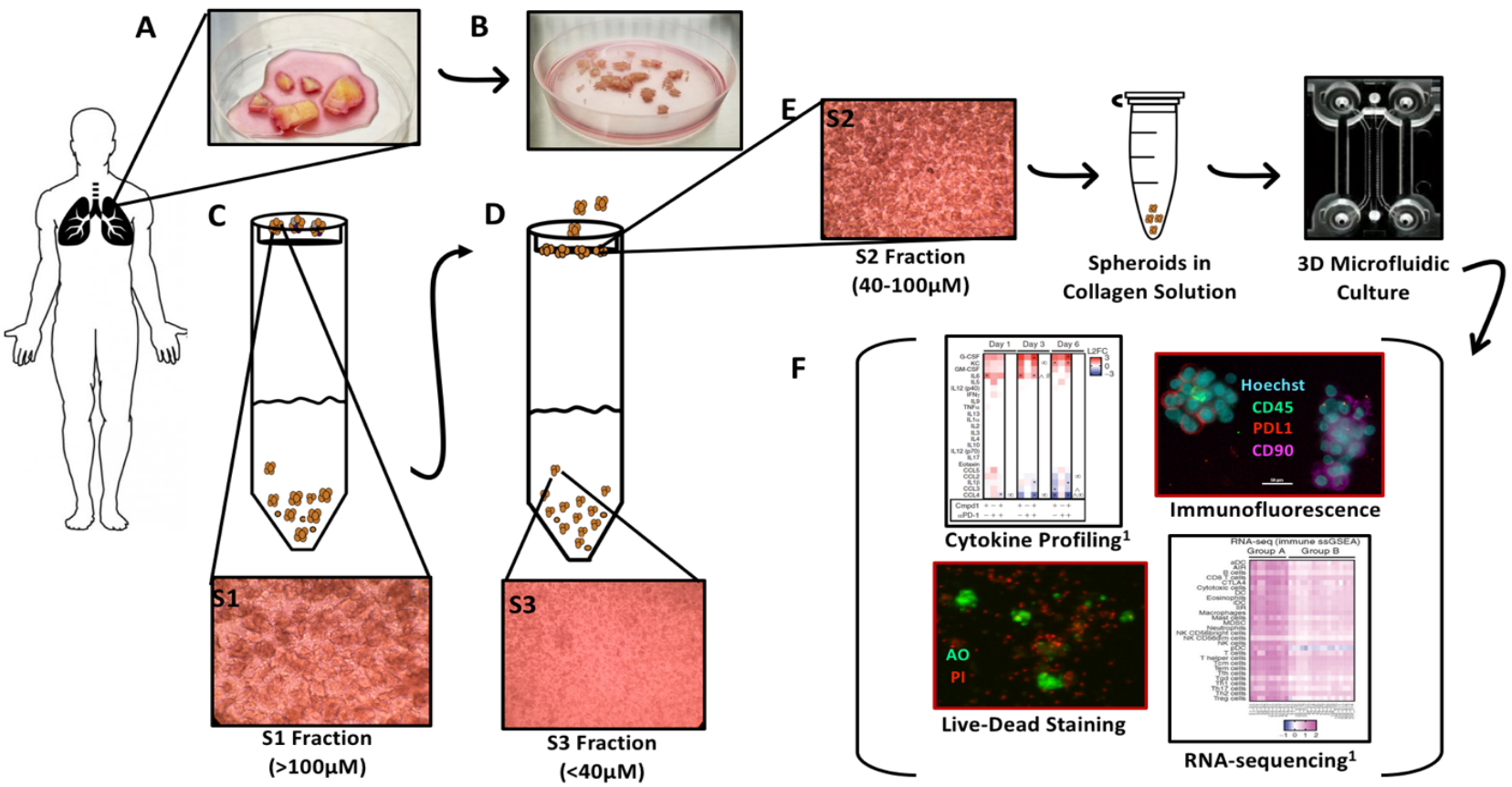

Figure 2. Generation of patient-derived organotypic spheroids (PDOTS).

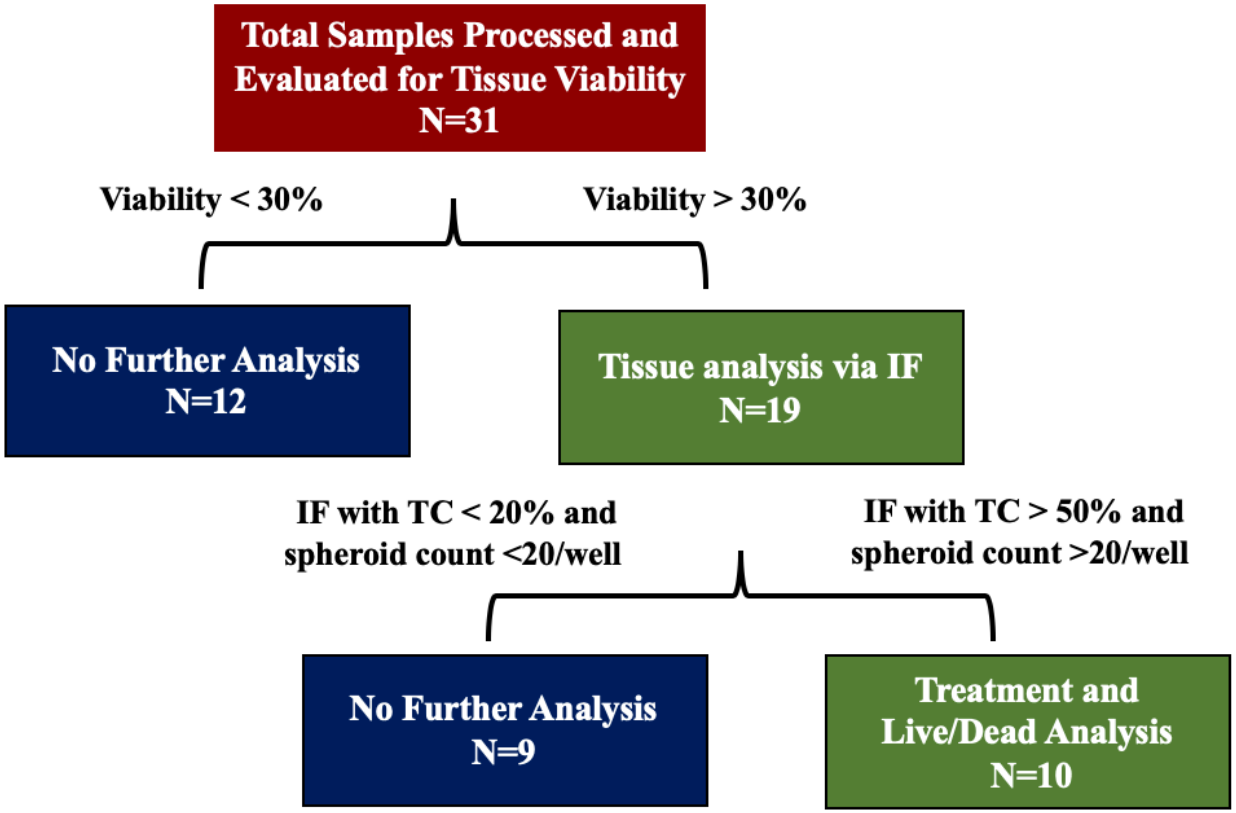

Figure 3. Inclusion and exclusion algorithm for processing of pleural specimens.

Mesothelioma Tissue Summary					
Mesothelioma Specimen #	**IF**	**Tumor Histology**	**Neoadjuvant Chemo**	**Post-Op Chemotherapy**	**Radiographic Tumor Response at Completion of Post-op Therapy**
5	50% Cell Viability 60% Tumor Content 20% CD90+ 60 CD8/well	Biphasic Sarcomatoid	None	**Salvage Therapy** Carb+Pem+Bev	No Response

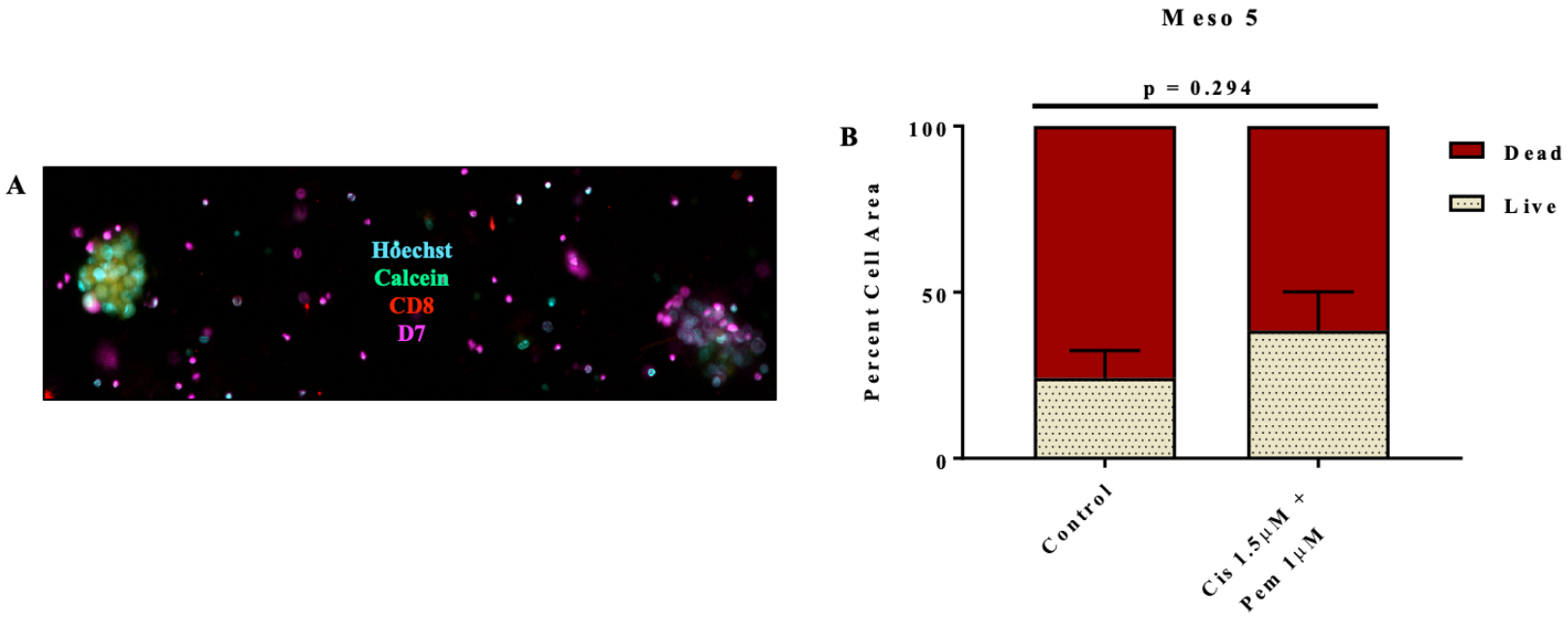

Figure 4. Mesothelioma specimen 5 | Immune profiling and *ex vivo* culture with concordant response *in vivo*

Mesothelioma Tissue Summary					
Mesothelioma Specimen #	**IF**	**Tumor Histology**	**Neoadjuvant Chemo**	**Post-Op Chemotherapy**	**Radiographic Tumor Response at Completion of Post-op Therapy**
7	60% Cell Viability 50% Tumor Content 10% CD90+ 50 CD8/well	Epithelioid	None	**Adjuvant Therapy** Carb + Pem	No tumor recurrence to date

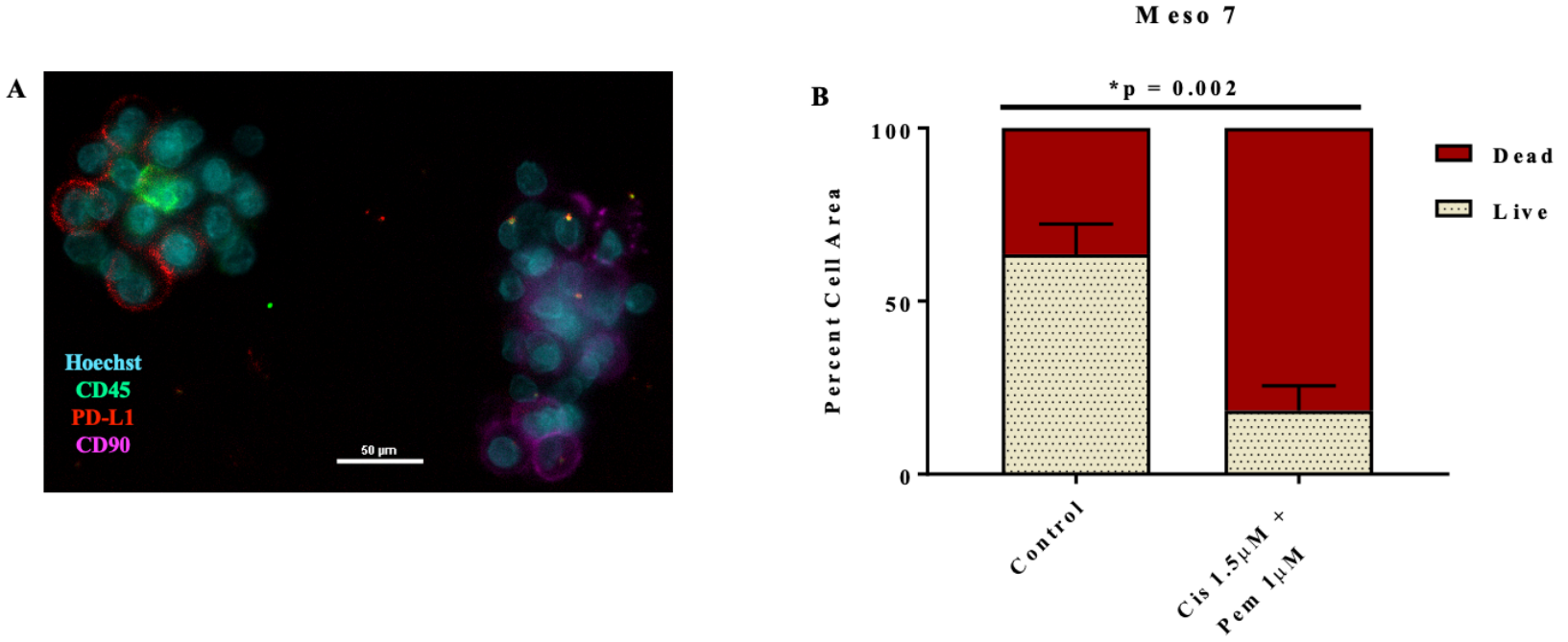

Figure 5. Mesothelioma specimen 7 | Immune profiling and *ex vivo* culture with concordant response *in vivo*

Mesothelioma Tissue Summary					
Mesothelioma Specimen #	**IF**	**Tumor Histology**	**Neoadjuvant Chemo**	**Post-Op Chemotherapy**	**Radiographic Tumor Response at Completion of Post-op Therapy**
15	30% Cell Viability 50% Tumor Content PD-L1 Negative Low CD8 Count	Biphasic - Epithelioid	None	**Adjuvant Therapy** Cis + Pem	No tumor recurrence to date

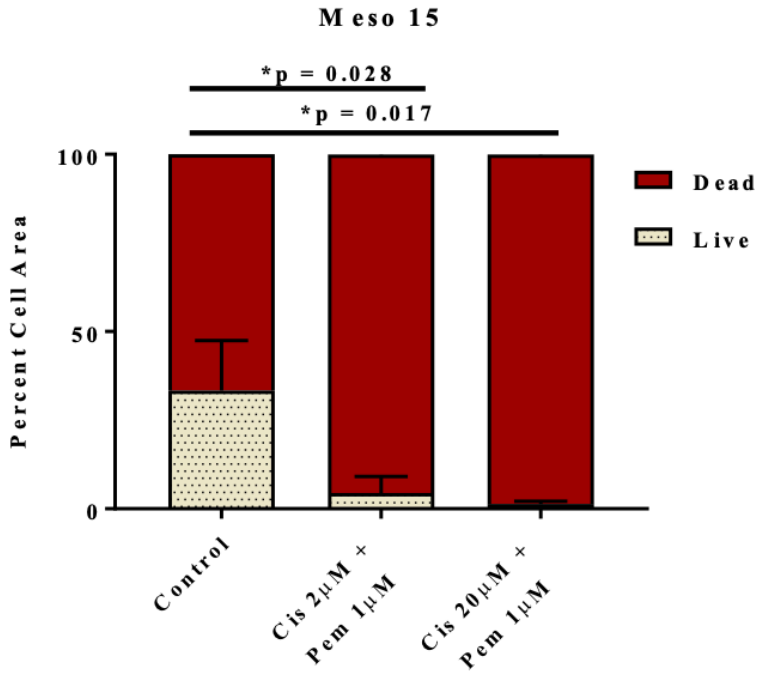

Figure 6. Mesothelioma specimen 15 | *Ex vivo* culture with varying cisplatin concentrations

Mesothelioma Tissue Summary					
Mesothelioma Specimen #	**IF**	**Tumor Histology**	**Neoadjuvant Chemo**	**Post-Op Chemotherapy**	**Radiographic Tumor Response at Completion of Post-op Therapy**
16	80% Cell Viability 90% Tumor Content 10% PD-L1 Positivity Low CD8 count	Biphasic - Epithelioid	None	**Adjuvant Therapy** Carb + Pem	No tumor recurrence to date

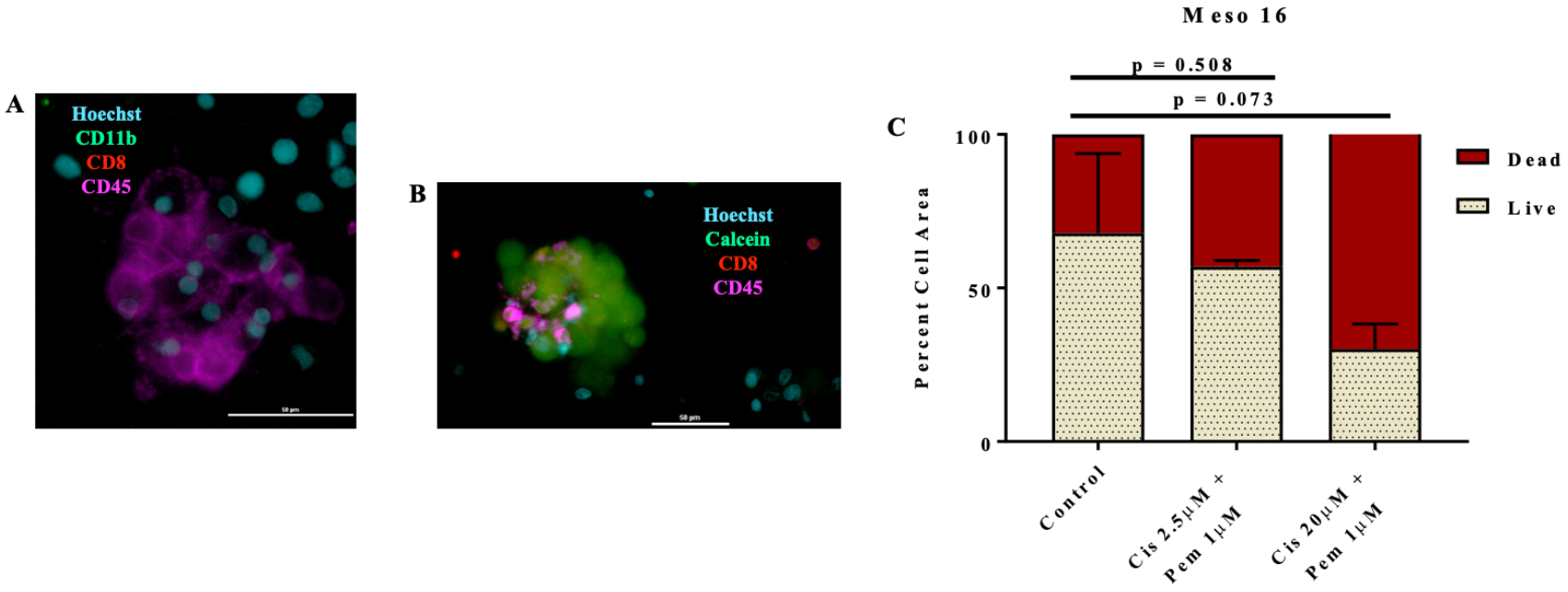

Figure 7. Mesothelioma specimen 16 | Immune profiling and *ex vivo* culture with discordant response *in vivo*

Mesothelioma Tissue Summary					
Mesothelioma Specimen #	**IF**	**Tumor Histology**	**Neoadjuvant Chemo**	**Post-Op Chemotherapy**	**Radiographic Tumor Response at Completion of Post-op Therapy**
14	50% Cell Viability 90% Tumor Content CD90 Negative PD-L1 Negative 30 CD8/well	Epithelioid	None	**Adjuvant Therapy** Carb + Pem	No tumor recurrence to date

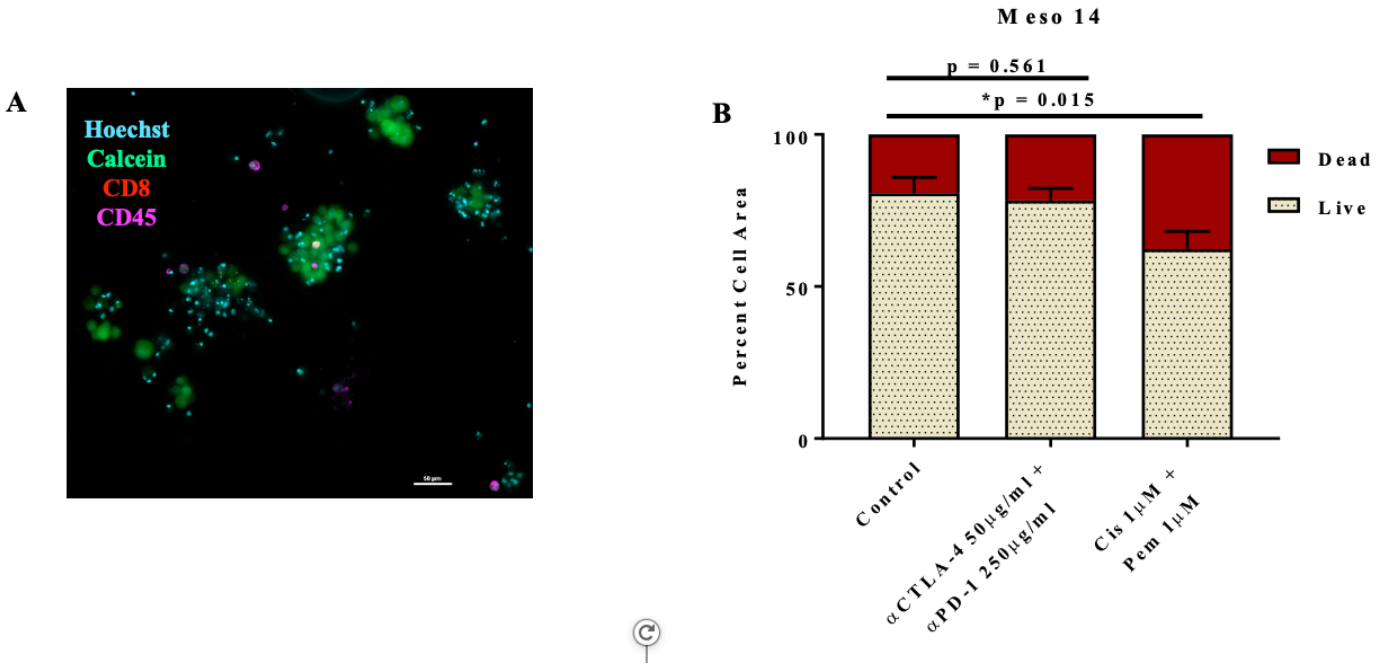

Figure 8. Mesothelioma specimen 14 | Immune profiling and *ex vivo* culture with immunotherapy and standard chemotherapy treatments

Table 1. Patient demographics and tissue characteristics of analyzed samples

	Total Patient Specimens N = 31	Untreated Specimens N=21	Treated Specimens N = 10	P-Value
Patient Age, years (mean)	69	69	68	0.583
Male Gender, n (%)	21 (68%)	14 (67%)	7 (70%)	0.999
Medical History, n (%)				
Asbestos Exposure	24 (77%)	17 (81%)	7 (70%)	0.652
Smoking History	16 (52%)	10 (48%)	6 (60%)	0.704
Pleurodesis before surgery, n (%)	5 (16%)	3 (14%)	2 (20%)	0.999
Treatment Status, n (%)				
Neoadjuvant Chemotherapy	11 (35%)	10 (48%)	1 (10%)	0.055
Surgery Performed, n (%)				
EPP	2 (6.5%)	2 (10%)	0	0.999
P/D	21 (68%)	12 (57%)	9 (90%)	0.106
Other	8 (26%)	7 (33%)	1 (10%)	0.222
Tumor Histology, n (%)				
Epithelioid	16 (52%)	10 (48%)	6 (60%)	0.704
Biphasic	15 (48%)	11 (52%)	4 (40%)	0.704

Abbreviations: EPP, Extrapleural pneumonectomy; P/D, Pleurectomy and decortication

Table 2. Analysis of cell viability and ischemic times based on treatment status of mesothelial tissue

A

Mesothelioma Specimen #	Neoadjuvant Chemotherapy	Tumor Histology	Warm : Cold Tissue Ischemia Time (min)	Viability	Tumor Content
17	No	Epithelioid	10	75%	60%
25	No	Epithelioid	11	80%	70%
16	No	Biphasic - Epithelioid	12	80%	90%
22	No	Epithelioid	22	90%	60%
10	No	Epithelioid	25	60%	75%
23*	No	Epithelioid	30	50%	50%
7	No	Epithelioid	45	60%	50%
4	No	Biphasic - Pleomorphic	40	50%	---
24	No	Epithelioid	56	60%	---
Average			**28 min**		

B

Mesothelioma Specimen #	Neoadjuvant Chemotherapy	Tumor Histology	Warm : Cold Tissue Ischemia Time (min)	Viability	Tumor Content
11*	Pem + Cis	Epithelioid	29	75%	80%
19	Pem + Cis	Epithelioid	29	<5%	---
21	Pem + Cis	Biphasic - Sarcomatoid	32	<5%	---
18*	Pem + Cis	Epithelioid	34	<5%	50%
1	Pem + Cis	Epithelioid	50	<10%	---
27*	Pem + Cis	Biphasic	55	<10%	---
6	Pem + Cis + Bev	Biphasic - Sarcomatoid	68	30%	---
3	Pem + Cis	Biphasic - Sarcomatoid	100	<10%	---
8	Pem + Cis	Epithelioid	195	<5%	---
Average			**66 min**		

C

Mesothelioma Specimen #	Neoadjuvant Chemotherapy	Tumor Histology	Warm : Cold Tissue Ischemia Time (min)	Viability	Tumor Content
9	No	Biphasic Epithelioid	16	20%	---
20	No	Epithelioid w/sarcomatoid feat.	20	<5%	---
26	No	Biphasic	30	20%	---
15*	No	Biphasic - Epithelioid	30	30%	50%
2	No	Biphasic - Sarcomatoid	72	<10%	---
Average			**34 min**		

Tumor samples positive for pleurodesis

Figure and Table Legends

Figures Legends

Figure 1. Tissue processing from the operating room to the lab bench

A. Surgical resection of tumor via P/D or EPP and collection of pleural specimens. B. Tissue processing and allocation by pathology department with noting of warm and cold ischemia times. C. Enzymatic and mechanical dissociation of pleural tissue. D. Generation of spheroids E. Spheroids in microfluidic culture device for subsequent *ex vivo* analysis.

Figure 2. Generation of patient-derived organotypic spheroids (PDOTs). A. Fresh patient tumor specimen in DMEM media. B. Specimen minced using sterile forceps and scalpel while suspended in collagenase solution C. S1 spheroid fraction of minced tumor strained over 100uM filter. D. S1 fraction flow through strained over 40uM filter to generate S2 and S3 spheroid fractions. E. S2 fraction used for *ex vivo* microfluidic culture. F. Implementable techniques following 3-7 days of culture.

Figure 3. Inclusion and exclusion algorithm for processing of pleural specimens

Algorithm outlining processing steps prior to specimen selection for treatment evaluation. Mesothelioma tissue specimens with viability greater than 15% underwent immunofluorescence analysis. During immunofluorescence characterization, tumor content of greater than 50% and spheroid count greater than 20 spheroids per well proceeded for further testing with standard chemotherapy and experimental treatments.

Figure 4. Mesothelioma specimen 5 | Immune profiling and *ex vivo* culture with concordant response *in vivo*

A. Immunofluorescence staining for immune cells and cell viability B. Live/dead analysis of spheroids performed on day 5 following treatment with media control and standard chemotherapy. Abbreviations: Bev, Bevacizumab; Carb, Carboplatin; Cis, Cisplatin; IF, Immunofluorescence; Pem, Pemetrexed

Figure 5. Mesothelioma specimen 7 | Immune profiling and *ex vivo* culture with concordant response *in vivo*

A. Immunofluorescence staining for immune cells and tumor content B. Live/dead analysis of spheroids performed on day 4 following treatment with media control and standard chemotherapy. Abbreviations: Carb, Carboplatin; Cis, Cisplatin; IF, Immunofluorescence; Pem, Pemetrexed

Figure 6. Mesothelioma specimen 15 | *Ex vivo* culture with varying cisplatin concentrations

Live/dead analysis of spheroids performed on day 4 following treatment with media control and standard chemotherapy with increased cisplatin dosing. Abbreviations: Cis, Cisplatin; IF, Immunofluorescence; Pem, Pemetrexed

Figure 7. Mesothelioma specimen 16 | Immune profiling and *ex vivo* culture with discordant response *in vivo*

A. Immunofluorescence staining for immune cells and cell viability B. Live/dead analysis of spheroids performed on day 4 following treatment with media control and standard chemotherapy with increased cisplatin dosing. Abbreviations: Carb, Carboplatin; Cis, Cisplatin; IF, Immunofluorescence; Pem, Pemetrexed

Figure 8. Mesothelioma specimen 14 | Immune profiling and *ex vivo* culture with immunotherapy and standard chemotherapy treatments

A. Immunofluorescence staining for immune cells and cell viability B. Live/dead analysis of spheroids performed on day 6 following treatment with isotype IgG control (10ug/ml), immunotherapy, and standard chemotherapy. Abbreviations: Carb, carboplatin; Cis, cisplatin; IF, Immunofluorescence; Pem, pemetrexed

Table Legends

Table 1. Patient demographics and tissue characteristics of analyzed samples

Patient demographics and tissue characteristics of specimens treated with standard chemotherapy (cisplatin and pemetrexed) in *ex vivo* culture compared to untreated samples. Total number of samples in this study are included for reference.

Table 2. Analysis of cell viability and ischemic times based on treatment status of mesothelial tissue

A. Pleural specimens with treatment naïve status B. Pleural specimens treated with neoadjuvant chemotherapy C. Sub-cohort of pleural specimens with treatment naïve status and low tissue viability.

References

1. Sterman DH, Litzky LA, Kaiser LR. Epidemiology of malignant pleural mesothelioma. Post TW, ed. UpToDate. Waltham, MA: UpToDate Inc. http://www.uptodate.com
2. Van schil PE, Baas P, Gaafar R, et al. Trimodality therapy for malignant pleural mesothelioma: results from an EORTC phase II multicentre trial. Eur Respir J. 2010;36(6):1362-9.
3. Krug LM, Pass HI, Rusch VW, et al. Multicenter phase II trial of neoadjuvant pemetrexed plus cisplatin followed by extrapleural pneumonectomy and radiation for malignant pleural mesothelioma. J Clin Oncol. 2009;27(18):3007-13.
4. Aisner J. Current approach to malignant mesothelioma of the pleura. Chest. 1995;107(6 Suppl):332S-344S.
5. Tsao AS, VogelzangN. Systemic treatment for unresectable malignant pleural mesothelioma. Post TW, ed. UpToDate. Waltham, MA: UpToDate Inc. http://www.uptodate.com
6. Teta MJ, Mink PJ, Lau E, Sceurman BK, Foster ED. US mesothelioma patterns 1973-2002: indicators of change and insights into background rates. Eur J Cancer Prev. 2008 Nov;17(6):525-34.
7. Survival Statistics for Mesothelioma. American Cancer Society. https://www.cancer.org/cancer/malignant-mesothelioma/detection-diagnosis-staging/survival-statistics.html. Published December 20, 2017. Accessed April 1, 2018.
8. Pass HI, Vogelzang NT, Hahn SM et al. Benign and malignant mesothelioma. In: DeVita VT, Hellman S, Rosenberg SA, eds. Cancer: principles and practice of oncology. 8th ed. Philadelphia: Lippincott, Williams & Wilkins; 2008:1835–62.
9. Price B, Ware A. Time trend of mesothelioma incidence in the United States and projection of future cases: an update based on SEER data from 1973 through 2005. *Crit Rev Toxicol.*2009; 39:576–88.
10. Metintas M, Ozdemir N, Hillerdal G, Uçgun I, Metintas S, Baykul C, Elbek O,Mutlu S, Kolsuz M. Environmental asbestos exposure and malignant pleural mesothelioma. Respir Med. 1999 May;93(5):349-55.

11. Pan XL, Day HW, Wang W, Beckett LA, Schenker MB. Residential proximity to naturally occurring asbestos and mesothelioma risk in California. Am J Respir Crit Care Med. 2005 Oct 15;172(8):1019-25.
12. Teta MJ, Lau E, Sceurman BK, Wagner ME. Therapeutic radiation for lymphoma: risk of malignant mesothelioma. Cancer. 2007 Apr 1;109(7): 1432-8.
13. Panou V, Gadiraju M, Wolin A, Weipert CM, Skarda E, Husain AN, Patel JD, Rose B, Zhang SR, Weatherly M, Nelakuditi V, Knight Johnson A, Helgeson M, Fischer D, Desai A, Sulai N, Ritterhouse L, Røe OD, Turaga KK, Huo D, Segal J, Kadri S, Li Z, Kindler HL, Churpek JE. Frequency of Germline Mutations in Cancer Susceptibility Genes in Malignant Mesothelioma. J Clin Oncol. 2018 Oct 1;36(28):2863-2871.
14. Bott M, Brevet M, Taylor BS, Shimizu S, Ito T, Wang L, Creaney J, Lake RA, Zakowski MF, Reva B, Sander C, Delsite R, Powell S, Zhou Q, Shen R, Olshen A, Rusch V, Ladanyi M. The nuclear deubiquitinase BAP1 is commonly inactivated by somatic mutations and 3p21.1 losses in malignant pleural mesothelioma. Nat Genet. 2011 Jun 5;43(7):668-72.
15. De Rienzo A, Tor M, Sterman DH, Aksoy F, Albelda SM, Testa JR. Detection of SV40 DNA sequences in malignant mesothelioma specimens from the United States, but not from Turkey. J Cell Biochem. 2002;84(3):455-9.
16. Sterman DH, Litzky LA, Kaiser LR. Presentation, initial evaluation, and prognosis of malignant pleural mesothelioma. Post TW, ed. UpToDate. Waltham, MA: UpToDate Inc. http://www.uptodate.com
17. Boutin C, Rey F, Gouvernet J, Viallat JR, Astoul P, Ledoray V. Thoracoscopy in pleural malignant mesothelioma: a prospective study of 188 consecutive patients. Part 2: Prognosis and staging. Cancer. 1993 Jul 15;72(2):394-404.
18. Creaney J, Francis RJ, Dick IM, Musk AW, Robinson BW, Byrne MJ, Nowak AK. Serum soluble mesothelin concentrations in malignant pleural mesothelioma: relationship to tumor volume, clinical J stage and changes in tumor burden. Clin Cancer Res 2011;17:1181–1189.
19. Luo L, Shi HZ, Liang QL, Jiang J, Qin SM, Deng JM. Diagnostic value of soluble mesothelin-related peptides for malignant mesothelioma: a meta-analysis. Respir Med 2010;104:149–156.

20. Schneider J, Hoffmann H, Dienemann H, Herth FJ, Meister M, Muley T., Dienemann H. Diagnostic and prognostic value of soluble mesothelin-related proteins in patients with malignant pleural mesothelioma in comparison with benign asbestosis and lung cancer. J Thorac Oncol. 2008;3:1317–1324.
21. Canessa PA, Franceschini MC, Ferro P, Battolla E, Dessanti P, Manta C, Sivori M, Pezzi R, Fontana V, Fedeli F, Pistillo MP, Roncella S. Evaluation of soluble mesothelin-related peptide as a diagnostic marker of malignant pleural mesothelioma effusions: its contribution to cytology. Cancer Invest. 2013 Jan;31(1):43-50.
22. Litzky LA. Pathology of malignant pleural mesothelioma. Post TW, ed. UpToDate. Waltham, MA: UpToDate Inc. http://www.uptodate.com
23. Ray M, Kindler HL. Malignant pleural mesothelioma: an update on biomarkers and treatment. *Chest.* 2009; 136:888–96.
24. Van Gerwen M, Alpert N, Wolf A, Ohri N, Lewis E, Rosenzweig KE, Flores R, Taioli E. Prognostic Factors of Survival in Patients with Malignant Pleural Mesothelioma; an analysis of the National Cancer Data Base. Carcinogenesis. 2019 Jan 10. doi: 10.1093/carcin/bgz004. [Epub ahead of print]
25. Brims FJ, Meniawy TM, Duffus I, de Fonseka D, Segal A, Creaney J, Maskell N,Lake RA, de Klerk N, Nowak AK. A Novel Clinical Prediction Model for Prognosis in Malignant Pleural Mesothelioma Using Decision Tree Analysis. J Thorac Oncol. 2016 Apr;11(4):573-82.
26. Musk AW, Olsen N, Alfonso H, Reid A, Mina R, Franklin P, Sleith J, Hammond N, Threlfall T, Shilkin KB, de Klerk N (2011) Predicting survival in malignant mesothelioma. Eur Respir J 38(6): 1420–1424.
27. Pass HI, Tsao AS, Rosenzweig K. Initial management of malignant pleural mesothelioma. Post TW, ed. UpToDate. Waltham, MA: UpToDate Inc. http://www.uptodate.com
28. Dasari S, Tchounwou PB. Cisplatin in cancer therapy: molecular mechanisms of action. *Eur J Pharmacol*. 2014;740:364-78.
29. Vogelzang NJ, Rusthoven JJ, Symanowski J, Denham C, Kaukel E, Ruffie P, Gatzemeier U, Boyer M, Emri S, Manegold C, Niyikiza C, Paoletti P. Phase III study of pemetrexed

in combination with cisplatin versus cisplatin alone in patients with malignant pleural mesothelioma. J Clin Oncol. 2003 Jul 15;21(14):2636-44.

30. Lang-Lazdunski L, Bille A, Lal R, Cane P, McLean E, Landau D, Steele J, Spicer J. Pleurectomy/decortication is superior to extrapleural pneumonectomy in the multimodality management of patients with malignant pleural mesothelioma. J Thorac Oncol. 2012 Apr;7(4):737-43.
31. Rena O, Casadio C. Extrapleural pneumonectomy for early stage malignant pleural mesothelioma: a harmful procedure. Lung Cancer. 2012 Jul;77(1):151-5.
32. Bovolato P, Casadio C, Billè A, Ardissone F, Santambrogio L, Ratto GB, Garofalo G, Bedini AV, Garassino M, Porcu L, Torri V, Pastorino U. Does surgery improve survival of patients with malignant pleural mesothelioma?: a multicenter retrospective analysis of 1365 consecutive patients. J Thorac Oncol. 2014 Mar;9(3):390-6.
33. Gupta V, Mychalczak B, Krug L, Flores R, Bains M, Rusch VW, Rosenzweig KE. Hemithoracic radiation therapy after pleurectomy/decortication for malignant pleural mesothelioma. Int J Radiat Oncol Biol Phys. 2005 Nov 15;63(4):1045-52.
34. Rosenzweig KE, Zauderer MG, Laser B, Krug LM, Yorke E, Sima CS, Rimner A, Flores R, Rusch V. Pleural intensity-modulated radiotherapy for malignant pleural mesothelioma. Int J Radiat Oncol Biol Phys. 2012 Jul 15;83(4):1278-83.
35. Minatel E, Trovo M, Polesel J, Rumeileh IA, Baresic T, Bearz A, Del Conte A, Franchin G, Gobitti C, Drigo A, Dassie A, Pagan V, Trovo MG. Tomotherapy after pleurectomy/decortication or biopsy for malignant pleural mesothelioma allows the delivery of high dose of radiation in patients with intact lung. J Thorac Oncol. 2012 Dec;7(12):1862-1866.
36. Rimner A, Spratt DE, Zauderer MG, Rosenzweig KE, Wu AJ, Foster A, Yorke ED, Adusumilli P, Rusch VW, Krug LM. Failure patterns after hemithoracic pleural intensity modulated radiation therapy for malignant pleural mesothelioma. Int J Radiat Oncol Biol Phys. 2014 Oct 1;90(2):394-401.
37. Allen AM, Czerminska M, Jänne PA, Sugarbaker DJ, Bueno R, Harris JR, Court L, Baldini EH. Fatal pneumonitis associated with intensity-modulated radiation therapy for mesothelioma. Int J Radiat Oncol Biol Phys. 2006 Jul 1;65(3):640-5.

38. Miles EF, Larrier NA, Kelsey CR, Hubbs JL, Ma J, Yoo S, Marks LB. Intensity-modulated radiotherapy for resected mesothelioma: the Duke experience. Int J Radiat Oncol Biol Phys. 2008 Jul 15;71(4):1143-50.
39. Cao C, Tian D, Manganas C, Matthews P, Yan TD. Systematic review of trimodality therapy for patients with malignant pleural mesothelioma. Ann Cardiothorac Surg. 2012;1(4):428-37.
40. Nowak AK. Chemotherapy for malignant pleural mesothelioma: a review of current management and a look to the future. *Annals of Cardiothoracic Surgery*. 2012;1(4):508-515.
41. Housman G, Byler S, Heerboth S, et al. Drug resistance in cancer: an overview. Cancers (Basel). 2014;6(3):1769-92.
42. Filipp FV. Precision medicine driven by cancer systems biology. Cancer Metastasis Rev. 2017;36(1):91-108.
43. Jenkins RW, Aref AR, Lizotte PH, Ivanova E, Stinson S, Zhou CW, Bowden M, Deng J, Liu H, Miao D, He MX, Walker W, Zhang G, Tian T, Cheng C, Wei Z, Palakurthi S, Bittinger M, Vitzthum H, Kim JW, Merlino A, Quinn M, Venkataramani C, Kaplan JA, Portell A, Gokhale PC, Phillips B, Smart A, Rotem A, Jones RE, Keogh L, Anguiano M, Stapleton L, Jia Z, Barzily-Rokni M, Cañadas I, Thai TC, Hammond MR, Vlahos R, Wang ES, Zhang H, Li S, Hanna GJ, Huang W, Hoang MP, Piris A, Eliane JP, Stemmer-Rachamimov AO, Cameron L, Su MJ, Shah P, Izar B, Thakuria M, LeBoeuf NR, Rabinowits G, Gunda V, Parangi S, Cleary JM, Miller BC, Kitajima S, Thummalapalli R, Miao B, Barbie TU, Sivathanu V, Wong J, Richards WG, Bueno R, Yoon CH, Miret J, Herlyn M, Garraway LA, Van Allen EM, Freeman GJ, Kirschmeier PT, Lorch JH, Ott PA, Hodi FS, Flaherty KT, Kamm RD, Boland GM, Wong KK, Dornan D, Paweletz CP, Barbie DA. Ex Vivo Profiling of PD-1 Blockade Using Organotypic Tumor Spheroids. Cancer Discov. 2018 Feb;8(2):196-215.
44. Carvalho MR, Lima D, Reis RL, Correlo VM, Oliveira JM. Evaluating Biomaterial-and Microfluidic-Based 3D Tumor Models. Trends Biotechnol. 2015;33(11):667-678.
45. Halldorsson S, Lucumi E, Gómez-Sjöberg R, Fleming RMT. Advantages and challenges of microfluidic cell culture in polydimethylsiloxane devices. Biosens Bioelectron. 2015 Jan 15; 63:218-231.

46. Aref AR, Huang RY, Yu W, Chua KN, Sun W, Tu TY, Bai J, Sim WJ, Zervantonakis IK, Thiery JP, Kamm RD. Screening therapeutic EMT blocking agents in a three-dimensional microenvironment. Integr Biol (Camb). 2013 Feb;5(2):381-9.
47. Aref AR, Campisi M, Ivanova E, Portell A, Larios D, Piel BP, Mathur N, Zhou C, Coakley RV, Bartels A, Bowden M, Herbert Z, Hill S, Gilhooley S, Carter J,Cañadas I, Thai TC, Kitajima S, Chiono V, Paweletz CP, Barbie DA, Kamm RD, Jenkins RW. 3D microfluidic ex vivo culture of organotypic tumor spheroids to model immune checkpoint blockade. Lab Chip. 2018 Oct 9;18(20):3129-3143.
48. Dutta D, Heo I, Clevers H. Disease Modeling in Stem Cell-Derived 3D Organoid Systems. Trends Mol Med. 2017;23(5):393-410.
49. Clevers H. Modeling Development and Disease with Organoids. Cell. 2016;165(7):1586-1597.
50. Byrne AT, Alférez DG, Amant F, et al. Interrogating open issues in cancer precision medicine with patient-derived xenografts. Nat Rev Cancer. 2017;17(4):254-268.
51. Micalizzi DS, Maheswaran S, Haber DA. A conduit to metastasis: circulating tumor cell biology. Genes Dev. 2017;31(18):1827-1840.
52. Däster S, Amatruda N, Calabrese D, Ivanek R, Turrini E, Droeser RA, Zajac P, Fimognari C, Spagnoli GC, Iezzi G, Mele V, Muraro MG. Induction of hypoxia and necrosis in multicellular tumor spheroids is associated with resistance to chemotherapy treatment. Oncotarget. 2017 Jan 3;8(1):1725-1736.
53. Farahat WA, Wood LB, Zervantonakis IK, Schor A, Ong S, Neal D, Kamm RD, Asada HH. Ensemble analysis of angiogenic growth in three-dimensional microfluidic cell cultures. PLoS One.2012;7(5):e37333.
54. R Core Team. *R: A Language and Environment for Statistical Computing*. (R Foundation for Statistical Computing, 2017).
55. Kawamura K, Hiroshima K, Suzuki T, Chai K, Yamaguchi N, Shingyoji M, Yusa T, Tada Y, Takiguchi Y, Tatsumi K, Shimada H, Tagawa M. CD90 is a diagnostic marker to differentiate between malignant pleural mesothelioma and lung carcinoma with immunohistochemistry. Am J Clin Pathol. 2013 Oct;140(4):544-9.
56. Zalcman G, Mazieres J, Margery J, Greillier L, Audigier-Valette C, Moro-Sibilot D, Molinier O, Corre R, Monnet I, Gounant V, Rivière F, Janicot H, Gervais R, Locher C,

Milleron B, Tran Q, Lebitasy MP, Morin F, Creveuil C, Parienti JJ, Scherpereel A; French Cooperative Thoracic Intergroup (IFCT).Bevacizumab for newly diagnosed pleural mesothelioma in the Mesothelioma Avastin Cisplatin Pemetrexed Study (MAPS): a randomised, controlled, open-label, phase 3 trial. Lancet. 2016 Apr 2;387(10026):1405-1414.

57. Andre F, Mardis E, Salm M, Soria JC, Siu LL, Swanton C. Prioritizing targets for precision cancer medicine. Ann Oncol. 2014 Dec;25(12):2295-303.
58. Roychowdhury S, Chinnaiyan AM. Translating genomics for precision cancer medicine. Annu Rev Genomics Hum Genet. 2014;15:395-415.
59. Sohal DP, Rini BI, Khorana AA, Dreicer R, Abraham J, Procop GW, Saunthararajah Y, Pennell NA, Stevenson JP, Pelley R, Estfan B, Shepard D, Funchain P, Elson P, Adelstein DJ, Bolwell BJ. Prospective Clinical Study of Precision Oncology in Solid Tumors. J Natl Cancer Inst. 2015 Nov 9;108(3).
60. Kunz-Schughart LA, Freyer JP, Hofstaedter F, Ebner R. The use of 3D cultures for high-throughput screening: the multicellular spheroid model. J Biomol Screen.2004 Jun;9(4):273-85.
61. Ho WJ, Pham EA, Kim JW, Ng CW, Kim JH, Kamei DT, Wu BM. Incorporation of multicellular spheroids into 3-D polymeric scaffolds provides an improved tumor model for screening anticancer drugs. Cancer Sci. 2010 Dec;101(12):2637-43.
62. Drewitz M, Helbling M, Fried N, Bieri M, Moritz W, Lichtenberg J, Kelm JM. Towards automated production and drug sensitivity testing using scaffold-free spherical tumor microtissues. Biotechnol J. 2011 Dec;6(12):1488-96.
63. Klebe S, Brownlee NA, Mahar A, Burchette JL, Sporn TA, Vollmer RT, Roggli VL. Sarcomatoid mesothelioma: a clinical-pathologic correlation of 326 cases. Mod Pathol. 2010 Mar;23(3):470-9.
64. Mansfield AS, Symanowski JT, Peikert T. Systematic review of response rates of sarcomatoid malignant pleural mesotheliomas in clinical trials. Lung Cancer. 2014 Nov;86(2):133-6.
65. Lievense LA, Sterman DH, Cornelissen R, Aerts JG. Checkpoint Blockade in Lung Cancer and Mesothelioma. Am J Respir Crit Care Med. 2017 Aug 1;196(3):274-282.

66. Topalian SL, Drake CG, Pardoll DM. Immune checkpoint blockade: a common denominator approach to cancer therapy. Cancer Cell 2015;27:450–61.
67. Dozier J, Zheng H, Adusumilli PS. Immunotherapy for malignant pleural mesothelioma: current status and future directions. *Transl Lung Cancer Res*. 2017;6(3):315-324.
68. Dumoulin, D.W.; Aerts, J.G.; Cornelissen, R. Is immunotherapy a viable option in treating mesothelioma? Future Oncol. 2017, 13, 1747–1750.
69. Eisenhauer EA, Therasse P, Bogaerts J, Schwartz LH, Sargent D, Ford R, Dancey J, Arbuck S, Gwyther S, Mooney M, Rubinstein L, Shankar L, Dodd L, Kaplan R,Lacombe D, Verweij J. New response evaluation criteria in solid tumours: revised RECIST guideline (version 1.1). Eur J Cancer. 2009 Jan;45(2):228-47.